

Characterization of a Turbine Airfoil Cooling Hole Check Standard for 5-axis CMMs - Uncertainty Reduction by Redundancy and Error Reversal

Joe Drescher, UTC - Pratt & Whitney, East Hartford, CT

Abstract

Measurement of the location of cooling holes generally requires a 5-axis, dual-sensor system. The size of the holes dictates an optical measurement while a touch probe is best to establish the location and orientation of the part. The measurement requires tilt and rotary axes to position the nominal hole axis parallel to the optical axis. Methods to certify volumetric performance of 5-axis, dual-sensor CMMs are not well established. One approach is the use of a check standard. This paper describes a sensitivity analysis approach to the estimate of task specific measurement uncertainty for the positions of holes on a check Standard. The mathematical model for the measurement is more complicated than is usually solved by this method [1].

1. Introduction

A check standard is to be used periodically as part of CMM calibration [2]. It has to be representative of all blades and stators to be inspected in terms of cooling hole size and configuration such that the full range of each machine axis is used in the check standard inspection. It was designed to have simple, prismatic geometry so that its coordinate system (CS) could be established accurately. Also, the holes were specified slightly larger than those in actual blades so that they could be produced with better form, thus reducing the measurement uncertainty related to this. Surface finish and optical properties were also targeted to match those of airfoil castings.

After the check standard was made, the first step was to measure the actual position of each hole. The uncertainty for the measurement had to be less than the capabilities of available 5-axis CMMs, that is, the machines to be tested. Traditional, bench layout was considered inadequate for all but the simplest hole location and orientation. An existing 5-axis CMM was chosen for the task with the expectation that special measurement methods could be used to improve the accuracy of results. The machine employs a standard touch-trigger probe to locate the part and a triangulation laser to locate each hole by edge detection. Multiple measurements and reversal techniques were used to reduce non-systematic and systematic components of measurement uncertainty, respectively, beyond what could have been achieved in a single measurement. Measurement uncertainty was estimated in two orthogonal directions for each of 44 holes. The 95% confidence interval ranged from a low value of 22.3 μ m to a high value of 36.8 μ m.

2. Measurement Method

The orientation of an airfoil in the hole measuring position is not unique. In general, there are two symmetrical and opposite orientations; clockwise (CW) and counterclockwise (CCW), corresponding to the tilt axis direction. The hole is measured as x-y true position in the hole CS defined such that Z is parallel to the nominal hole centerline.

Each measurement includes in each direction:

- The actual deviation of the hole position from nominal.
- Non-systematic error specific to CW or CCW orientation.
- Systematic errors specific to CW or CCW orientation.
- Systematic errors common to CW and CCW orientation.

The last group of errors is substantial in the dual-probe, 5-axis system. They include

- Datum of the measurement probe in the machine CS.
- Zero setting of linear axes.
- Zero setting of rotary and tilt axes.
- Coincidence error of two rotational average axes of rotation.
- Perpendicularity of Z axis to XY measurement plane.
- Parallelism of tilt axis to XY measurement plane.
- Perpendicularity of rotary and tilt axes of rotation.
- Various parametric errors of axes that do not move from CW to CWW orientation.

These were eliminated from the measurement error by the decision to measure both CW and CCW and calculate the hole position as half the difference of the positions measured in each direction. The actual deviation from nominal switches sign along with the part CS as it is rotated by 180 degrees within the machine CS while these bias terms do not switch sign.

The same errors, however, also occur during probing of the part to establish the part CS with respect to machine CS and therefore are not completely eliminated from the measurement results. They switch sign along with the measurand from CW to CCW during subsequent measurement. For the check standard, a simple change to the probing algorithm was adopted. It was probed in two mirror image sequences and the results of displacements and rotations of the two determined part CS were averaged. This eliminated the systematic errors that were common to both mirror image positions during part probing.

3. Analysis

Error in measurement, ε , then included all nonsystematic errors lumped together, NSE , the systematic errors of probing after reversal, PE' , the systematic errors of hole measurement after reversal, ME' , and the errors due to laser probe, part, sampling method, fitting and the interactions, $PPSFE$.

$$\varepsilon = NSE + PE' + ME' + PPSFE \quad (1)$$

The four terms were assumed linearly independent. That is, the components of error that would cause PE and ME to be correlated (the bias terms listed above) were simply neglected in the definitions of PE' and ME' . The expression for combined standard uncertainty is:

$$u^2(\varepsilon) = u^2(NSE) + u^2(PE') + u^2(ME') + u^2(PPSFE) \quad (2)$$

3.1 Standard Uncertainty due to nonsystematic errors

The nonsystematic error was estimated statistically from 10 measurement sets with $n = 10$, and estimate of standard deviation, s .

$$u^2(NSE) = s^2 / n$$

The standard uncertainty due to nonsystematic errors was calculated to be from 0.41 μm to 4.3 μm .

3.2 Standard Uncertainty due to errors during probing

For the final probing iteration, uncertainty was estimated for each measured deviation contained in \mathbf{P} , a 1X6 matrix of the probe deviations measured from the nominal, expected location. The check standard is shown in Figure 1 with the 6 probe points and their surface normal vectors numbered 1-6. It is a simple plane (1-3), line (4,5), point (6) system.

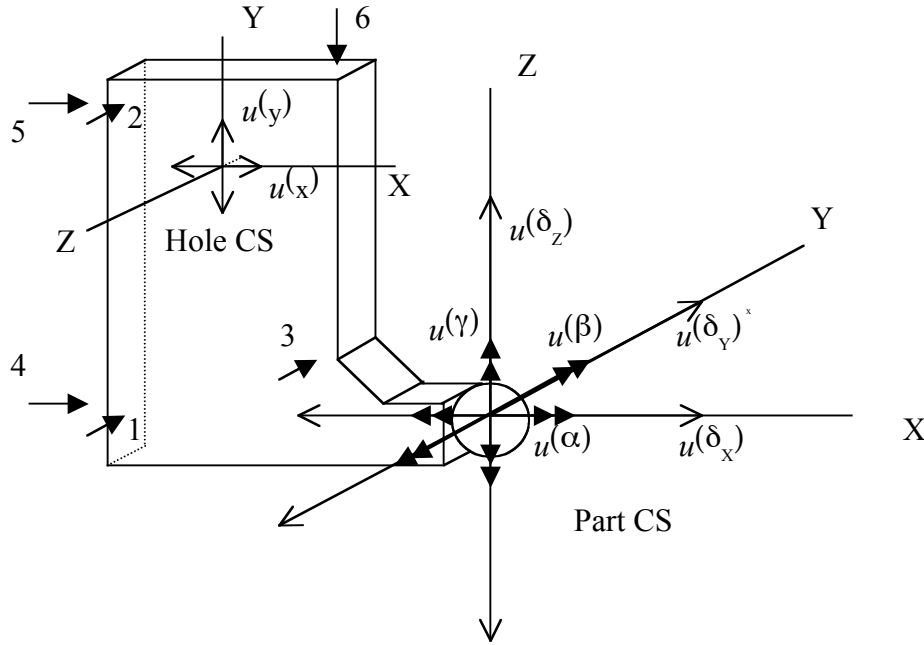


Fig. 1. The check standard artifact schematic showing probe points, nominal part CS, and deviations of part CS from nominal.

The standard uncertainty of each probe deviation was estimated using guidelines for estimating uncertainty [3]. Unknown, systematic machine errors were modeled with uniform probability and limits as measured during machine calibration. Appropriate fixed offsets were included taking into account the part geometry and location of the probe point relative to lines of measurement in the pre-process metrology. The list of unknown, systematic errors excluded those common to the symmetrical probing orientation. So, for example:

$$u^2(P_j) = \frac{n}{3} \sum_{i=1}^n \left(\frac{R_i}{2} OF_i \right)^2 \quad (3)$$

where:

R_i was the range of each error from the initial metrology.
 OF_i was the offset factor including unit conversion.

The offset factor was nonzero for X-Y squareness, A-axis angular accuracy and Y-axis pitch for the 1st probe point in the Y direction. Other error parameters included Y-axis linear accuracy and X-axis straightness. Equation (3) was applied to each of the 12 probe points, 6 in the cw and 6 in the ccw orientation.

Six parameters describing the deviation from nominal of the part CS are functions of the six probe deviations, $P_1, P_2, P_3, P_4, P_5,$ and P_6 contained in \mathbf{P} for both cw and ccw probe sequences. The three translations and three rotations may be written as $\mathbf{D} = [\delta x \ \delta y \ \delta z \ \alpha \ \beta \ \gamma]^T$. Uncertainties for these parameters were estimated by rules for propagation of uncertainty using the coefficient matrix, \mathbf{C} 6X6, where,

$$\mathbf{D} = \mathbf{C} (\mathbf{P}_{cw} + \mathbf{P}_{ccw}) \quad (4)$$

\mathbf{C} is comprised of part coordinates of the probe points. For example, angular deviation, α , of the part CS about the nominal X direction in expanded form is given by:

$$\alpha = \frac{1}{2} \left[\frac{1}{Z_2 - Z_1} (P_{1cw} + P_{1ccw}) - \frac{1}{Z_2 - Z_1} (P_{2cw} + P_{2ccw}) \right] \quad (5)$$

Clearly the errors in measured deviations at probe points may be correlated. Correlation coefficients were established by Monte Carlo simulation. Ranges of machine errors from pre-process metrology were taken as limits on uniform probability distributions with proper offsets applied to angular terms. Many sets of errors were generated to estimate possible probing error at each point by summation of individual errors and the correlation coefficient was calculated using the spreadsheet function. Thus the standard uncertainty was estimated for each parameter describing the location and orientation of the part CS.

The six uncertainty terms associated with the part CS were then transformed into each hole CS. The standard uncertainties of translation of the part CS origin were transformed directly into the hole CS by the two appropriate rotations for each hole. The standard uncertainties of orientation of the part CS were individually used to first calculate a translational uncertainty at the hole location in the part CS. This was then transformed into the hole CS through the appropriate angles. The standard uncertainty due to probing in X and Y directions of the hole CS as shown in Figure 1 was then the combination of the six terms taken as independent. This value ranged from 1.8 μm to 7.5 μm .

3.3 Standard Uncertainty due to errors during measurement

The reversal method, i.e. taking the measurement results as half the difference between CW and CCW results, eliminated many systematic errors. The remaining systematic errors as measured in the initial machine calibration were used to calculate the measurement uncertainty at each hole location. There was assumed to be no correlation between CW and CCW errors for any holes. In all but a few instances, tilt, rotary, X and Y axes all change position between the two mirror image orientations. Therefore, the standard uncertainty in each direction for each hole was taken as the combination of standard uncertainties of

individual machine errors. Again, these were modeled as having uniform probability distributions with bounds equal to the measured ranges. The standard uncertainty due to errors during measurement ranged from a low estimate of 1.6 μm to a maximum of 3.1 μm .

3.4 Part, probe, sampling, fitting interactions

A laser is focused to a nominal 80 μm spot and this is positioned to the nominal center of the hole. A preliminary 4 point edge finding sequence adjusts the center. The measurement then consists of 6 radial moves from the new center at 60 degree increments. A threshold intensity on the central area of the ccd array triggers a capture of the machine position at the hole edge. A least squares fit to the six points yields the measured center. Error sources include:

1. Edge condition such as debris and burrs
2. Velocity / effective radius / center start effects
3. CCD resolution
4. Laser shape at focus
5. Laser / detector asymmetry
6. Actual angle of the centerline of the cylinder (hole)
7. Hole roundness
8. Finite sampling

Items 1, 2, and 3 may be considered nonsystematic effects. They contribute to repeatability and are included in the NSE term. The shape of the laser was observed to have a symmetrical, elliptical cross section aligned with the machine axes. Therefore, because the primary measurement is the hole center and not size, this error was not included in the analysis. The laser detector asymmetry and angle of the hole were assumed to be eliminated by the measurement of each hole at 0 and 180 degrees (Reversed). The asymmetry of the single, 25degree detector angle may result in a smaller effective radius as the probe moves in the direction away from the detector. Light may be captured returning from the ID of the cylinder wall. The effect should be captured to some extent in the probe calibration and also it should be canceled in the reversal because the measurement is center position, not hole size. A similar effect may be caused when the angle of the cylinder varies from nominal and a similar argument may be made that this effect should be eliminated by the reversal.

The form error of the holes was observed to be significant considering the finite sampling of 6 edge positions to determine the center. Nine holes representing various positions and angles were measured using a modified probe routine with 60 points. The least squares center of the higher resolution edge profile was compared to the center using only the six points. A standard deviation was calculated from the 18 differences (9 x values and 9 y values) and this was used as the standard uncertainty due to part, probe, sampling, and fitting on all holes. $u(PPSFE) = 4.9\mu\text{m}$

4 Results and verification

The combined standard uncertainty from equation (2) with a coverage factor of 2 was used for the error bars about the average measurement. This is plotted in Figure 2. The maximum expanded uncertainty is 36 μm and the minimum is 22 μm . The check standard artifact was used to test three competing CMMs for a new equipment order. Some of the holes were

also checked by bench layout techniques. These four sets of independent data are also included in Figure 2. All data is normalized to the calibration results.

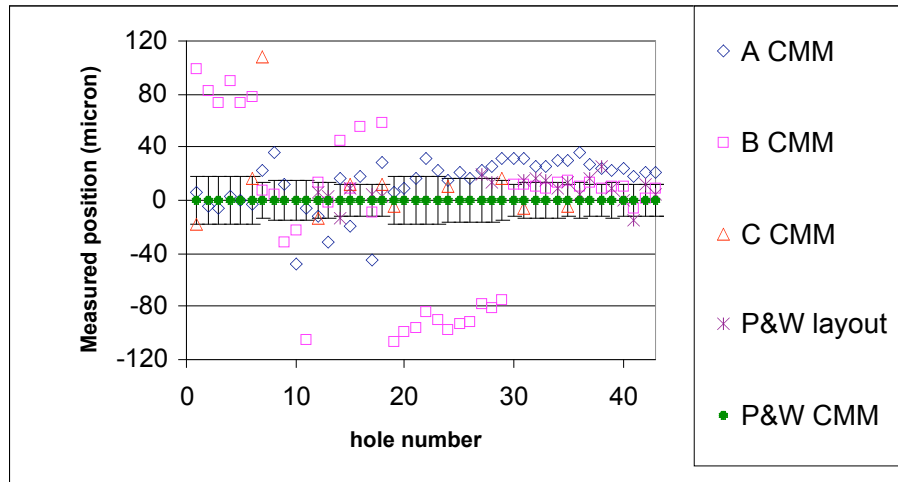


Fig. 2. Measurement results with expanded uncertainty shown by error bars and compared to four independent sets of measurements. P&W CMM measurements are set to zero and all others are shown as deviations.

5. Discussion

A few things should be analyzed to refine the uncertainty analysis. Treatment of the unknown, systematic squareness terms as uniformly distributed between specified bounds is not conservative. If the actual value is near one limit as is likely, the magnitude of the covariance term calculated by the simulation is too low. If squareness is large compared to the other errors, the CW and CCW results would be more highly correlated than estimated here. The best method is probably to correct the measurements for squareness although this is not trivial considering the part probing and measurement methods used.

Roll of X-axis and Y-axis were considered negligible as all measurement points were within 25mm of the line of straightness measurement. These terms may be added to a refined analysis.

The possible interactions between the laser probe system and the condition of the hole edges could be analyzed more fully. There are significant differences in the sensitivity to this between the laser probing method, optical contrast imaging and analysis, and manual measurement of pins.

References

- [1] Wilhelm R.G, Hocken R, Schwenke, H. Task Specific Uncertainty in Coordinate Measurement. Ann CIRP 2001;50/2:553-63
- [2] NCSL Z540.1. Calibration laboratories and measuring and test equipment. 1994
- [3] ISO Guide. Guide to the expression of uncertainty in measurement. ISBN 1993;92-67-10188-9